Vol 13 No 9, September 2004
1009-1963/2004/13(09)/1454-06

Chinese Physics

© 2004 Chin. Phys. Soc.
and IOP Publishing Ltd

Analysis of tunable picosecond pulse generation from a distributed feedback Ti:sapphire laser*

Hong Zhi(洪 治)† and Yao Xiao-Ke(姚小科)

State Key Laboratory of Modern Optical Instrumentation, Zhejiang University, Hangzhou 310027, *China*

(Received 29 December 2003; revised manuscript received 5 April 2004)

A distributed feedback Ti:sapphire laser (DFTL) pumped by a 532nm Q-switched pulse is proposed for the generation of tunable picosecond pulses. With coupled rate equation model, the temporal characteristics of DFTL are obtained. The numerical solutions show that the DFTL pulse with a 50-ps pulse duration and as much as 3.5mJ pulse energy can be obtained under 40-mJ, 5-ns pulse pumping. The dependence of output pulse width on the laser crystal's length, pumping pulse duration, and pumping rate is also discussed in detail.

Keywords: picosecond pulse, distributed feedback, Ti:sapphire laser, tunable
PACC: 4260B

1. Introduction

Tunable picosecond laser sources are practically important for a wide range of applications, such as time-resolved spectroscopy,[1,2] optical measurements,[3] optical sensing,[4] deployment in optical networks,[5] etc. Generally, these laser sources can be achieved through a technique known as mode-locking. Commercial laser products, for example, mode-locked Ti:sapphire lasers made by Spectra-Physics, have been developed to meet the foregoing applications. However, the applications of them are limited due to the following two reasons. One is that such kinds of lasers with mode-locking techniques, no matter whether active or passive,[6−8] even with cavity dumping,[9] need a complex and critical experimental setup; and the other is that the output energy is very small, around several tens of nJ if without amplifier.[10]

Distributed feedback (DFB) lasers provide a simple solution for the generation of tunable picosecond laser pulses. In 1980, Bor[11] constructed a DFB dye laser (DFDL) system, and the generation of tunable, nearly transform-limited single pulses with 36ps duration (FWHM) was achieved. A microchip-laser-pumped DFB-polymer-dye laser could produce much more shorter pulses with a duration of 13ps.[12] Recently, a DFDL with two amplifiers has been reported to have a pulse duration of 100ps and 3mJ pulse energy, and its wavelength is stabilized to within ±0.8pm in the visible range.[13] However, no tunable picosecond DFB lasers with other active media have been reported up to now.

Ti:sapphire lasers are widely used due to its wide tunability in the visible and near-infrared range. In this paper, we propose an experimental setup of DFTL for generating tunable picosecond laser pulses, the temporal behaviour of DFTL is obtained according to the theoretical model of coupled rate equations. The solution shows that single laser pulses with duration of about 66ps at high peak power of 40MW can be achieved without amplifier, and multiple pulses can be achieved with higher pumping rates. Based on the solution of numerical study, the pulse buildup behaviour and the pulse duration dependence of the laser crystal's length, pumping pulse duration, and pumping rate are discussed in detail.

2. Experimental setup

DFB laser action is made possible by the presence of periodic perturbations in the gain medium that provides feedback by backward Bragg scattering. The periodic perturbations can be induced by the

*Project supported by the National Natural Science Foundation of China (Grant No 60078002).
†E-mail: hongzhi@cise.zju.edu.cn

spatial modulation of the refractive index, or gain, or a combination of both, and they can be permanent, or transient. Picosecond laser action of a DFB laser is usually generated by spatial transient gain modulation in the active medium, which is induced by crossing two Q-switched pump beams to form interference fringes. The experimental setup of tunable picosecond Ti:sapphire DFB laser is quite similar to that in Ref.[11] (see Fig.1). The output beam from a Q-switched frequency-doubled Nd:YAG laser (532nm wavelength) is separated equally into two beams by diffraction of a holographic grating, then by crossing these two beams in the Ti:sapphire crystal with two reflection mirrors, a gain grating in the crystal is formed. The main advantage of the setup with a holographic grating is that good visibility of the interference fringes can be expected even if a low spatial coherence of pumping laser is used. The difference of our experimental arrangement from the above one is that a prism bonded to the laser crystal is introduced in order to satisfy the first-order Bragg effect.

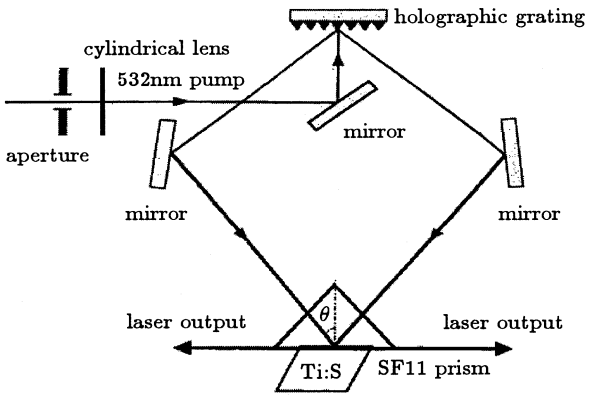


Fig.1. Experimental arrangement of a DFB Ti:sapphire laser for tunable picosecond pulse generation.

The output wavelength of a DFB laser satisfies the Bragg condition

$$\lambda_0 = \frac{2n_0\Lambda}{M}, \tag{1}$$

where λ_0 is the output wavelength in vacuum and lies in the range of 0.6–1.1μm due to active medium, n_0 is the refractive index of Ti:sapphire crystal (n_0=1.76), Λ is the modulation period, and M is the order of Bragg effect; first-order or second-order Bragg effect can be used in laser devices. Usually, the two diffracted beams from the holographic grating will be irradiated with an intersection angle 2θ on the laser crystal directly without a prism, and thus Λ is given by

$$\Lambda = \frac{\lambda_p}{2\sin\theta}, \tag{2}$$

where $\lambda_{\rm p}$ is the pumping wavelength of 532nm.

From Eqs.(1) and (2) we can obtain

$$\lambda_0 = \frac{n_0\lambda_{\rm p}}{M\sin\theta}. \tag{3}$$

For the second-order Bragg effect (M=2), the above tuning condition is easily satisfied by adjusting appropriate θ, the experimental arrangement is simple, but results in much higher threshold and lower efficiency, as compared with the first-order Bragg DFB lasers. As the first-order Bragg effect is considered in the experiment, a prism of SF11 (its refractive index n_1=1.795) bonded closely to the Ti:sapphire crystal (see Fig.1) is introduced to change the period of gain modulation, then the tunable output wavelength can be rewritten as

$$\lambda_0 = \frac{n_0\lambda_{\rm p}}{n_1\sin\theta}. \tag{4}$$

Therefore, the output radiation tuning in the whole active media spectrum can be easily achieved by tilting the fold mirrors about a vertical axis. It is important to ensure that there is no air interface between the prism and the laser crystal, otherwise the pumping beams would be totally reflected by bottom side of the prism.

3. Rate equations and their solution

3.1. Rate equations

Given that the Ti:sapphire laser can be represented by an ideal four-level system, the following rate equations can be used to study the temporal characteristics of DFTL:

$$\frac{{\rm d}n}{{\rm d}t} = I_{\rm P}\sigma_{\rm a}(N-n) - \frac{\sigma_{\rm e}c}{\eta}nq - \frac{n}{\tau}, \tag{5}$$

$$\frac{{\rm d}q}{{\rm d}t} = \frac{\sigma_{\rm e}c}{\eta}nq - \frac{q}{\tau_{\rm c}}, \tag{6}$$

where

N is the doping content of Ti ions,

n is the average concentration of Ti ions in the first excited singlet state,

q is the concentration of DFTL photons,

$\sigma_{\rm a}$ and $\sigma_{\rm e}$ are the absorption and stimulated emission cross-sections of Ti ions at the pumping and lasing wavelengths, respectively,

τ is the fluorescence lifetime in the absence of stimulated emission,

c is the speed of light at vacuum,

η is the average refractive index of the Ti: sapphire,

$I_{\rm p}$ is the average pump photon flux per unit area,

$\tau_{\rm c}$ is the equivalent cavity decay time.

In this model, we have neglected the excited state absorption, spontaneous emission, etc. The bleaching effect of ground state has been taken into consideration because of the considerable ratio of n and N, as will be shown in Section 3.2. Generally, when the pumping beams are within the near-field size, the excited region can be treated as a uniform transversely pumped cuboid of length L, height b, and depth a. Taking the e^{-1} penetration depth,

$$a = \frac{1}{N\sigma_{\rm a}}, \tag{7}$$

the equivalent cavity decay time, which is defined as the total photon number divided by the rate of photon loss, is given by[11]

$$\tau_{\rm c}(t) = \frac{\eta L^3}{2c\pi^2}\left[\left(\frac{\pi}{\lambda_0}\eta_1(t)\right)^2 + \left(\frac{1}{2M}\alpha_1(t)\right)^2\right], \tag{8}$$

where $\eta_1(t)$ and $\alpha_1(t)$ are the amplitudes of the spatial modulation of the refractive index and of the gain coefficient, respectively. In the case of DFTL, the first term in the right-hand side of Eq.(8) can be neglected and the spatial modulation of the gain can be easily calculated as

$$\alpha_1(t) = \sigma_{\rm e} V n(t), \tag{9}$$

where V is the visibility of the interference pattern. Thus, from Eqs.(8) and (9) we can have

$$\tau_{\rm c}(t) = \frac{\eta L^3 V^2 \sigma_{\rm e}^2}{8c\pi^2} n(t)^2, \tag{10}$$

for the first-order Bragg effect. The output power from one end of the DFTL is calculated to be

$$P_{\rm output}(t) = \frac{1}{2} \times \frac{hc}{\lambda_0} \times \frac{q(t)Lab}{\tau_{\rm c}(t)}. \tag{11}$$

In Eq.(11), q and $\tau_{\rm c}$ are time-dependent and $\tau_{\rm c}(t) - n(t)^2$. Therefore, in solving the coupled rate equations we will concentrate on the values of $q(t)$ and $n(t)$ and their effects on the output characteristics.

3.2. Solutions of rate equations

By assuming $\mathrm{d}q/\mathrm{d}t = 0$ the threshold value of the excited singlet state population $n_{\rm th}$ can be calculated from Eqs.(6) and (10):

$$n_{\rm th} = \frac{2}{\sigma_{\rm e} L}\left(\frac{\pi}{V}\right)^{2/3}. \tag{12}$$

This is a good reference to detailed numerical study. According to Table 1, we gain $n_{\rm th}$=1.13×10^{19}, i.e. 23% of doping content N, which is the reason that we have taken the bleaching effect of the ground state into the model. According to Refs.[14]–[17], from Eq.(12) we can easily derive the result that the DFTL is overcoupled when the laser system is operated on its threshold condition. This is consistent with the coupled rate equations which are derived from the overcoupled assumption.

Equations (5), (6), (10), and (11) are solved by using a fourth-order Runge–Kutta method corresponding to the condition given by Table 1. The numerical results are stable if the initial values of $n(t_0)$ and $q(t_0)$ are much smaller than $n_{\rm th}$ and the starting time t_0 is chosen at the point where $I_{\rm P}\,(t_0)$ is much less than the peak of $I_{\rm P}\,(t)$. Figure 2 shows the plots of computer solutions for different pumping rates. The stationary threshold of the first excited population indicated by the plots of $n(t)$ is verified by $n_{\rm th}$ which we have deduced above. The resolution indicates the generation of a series of picosecond pulses with decreasing amplitude. With increasing pump power, the number of pulses increases and the time separation between them decreases. In Fig.3, we can see that the peak power of pulses increases with the pumping rate. And in a certain region of pumping rates, single picosecond pulse is generated. The output peak power and duration of the single pulse versus pumping peak power are shown in Fig.4.

Table 1. Spectral parameters of Ti:sapphire used in the rate equations.

$N = 5 \times 10^{19}\mathrm{cm}^{-3}$, $\sigma_{\rm a} = 9.3 \times 10^{-20}\mathrm{cm}^2$, $\sigma_{\rm e} = 3.8 \times 10^{19}\mathrm{cm}^2$, $\tau = 3.2\mu$s,
λ_0=790nm, $\lambda_{\rm p}$=532nm, η=1.76, V=1, L=1cm, b=0.02cm,
Gaussian pumping pulse shape, pumping pulse duration=5ns

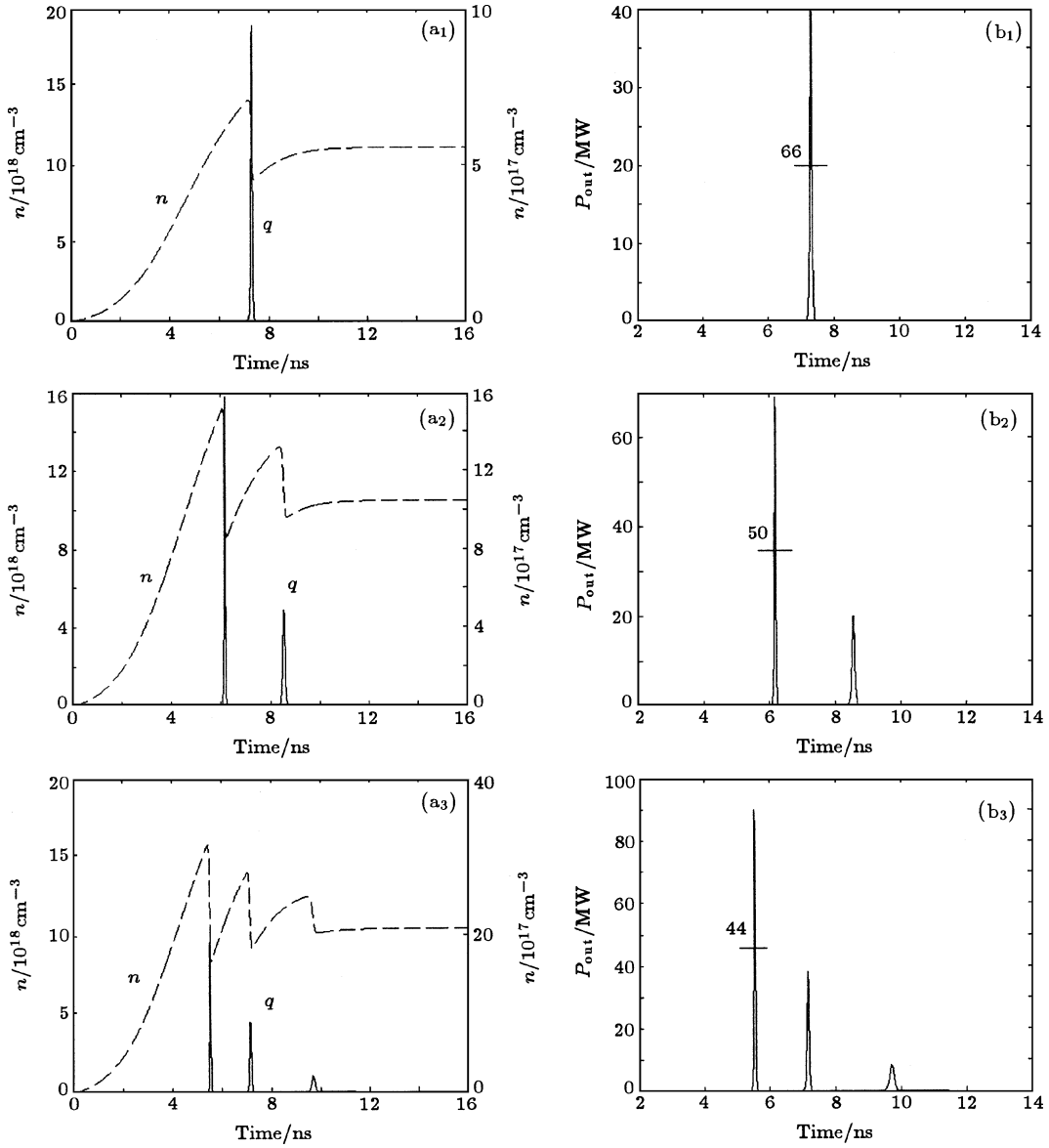


Fig.2. Computer solutions of the coupled rate equations. (a) Population of the first excited singlet state (n) and population of the photons (q); (b) output power of the DFB Ti:sapphire. The first pulse durations in picoseconds are also indicated. Subscripts 1–3 of a and b represent the different pumping peak powers (6, 8, and 10MW, respectively). A pumping power of 1MW corresponds to a pumping rate $I_{\mathrm{P}}\sigma_{\mathrm{a}}N = 6.23 \times 10^{26}\mathrm{cm}^{-3}\mathrm{s}^{-1}$.

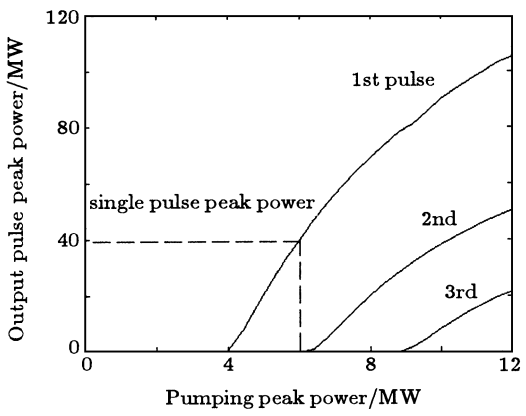


Fig.3. Calculated output peak power versus pumping peak power. The parameters for the calculations are the same as those in Fig.2.

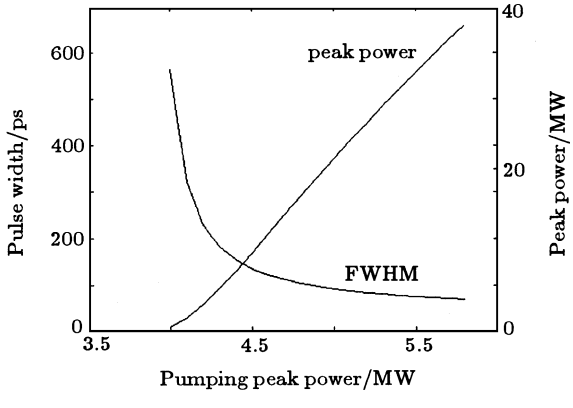


Fig.4. Calculated single pulse peak power and pulse duration (FWHM) versus pump power. The parameters for the calculations are the same as those in Fig.2.

The above temporal characteristics of DFTL are quite similar to DFDL. The most important characteristic of DFTL we are concerned with is the generation of picosecond pulses. We describe below the pulse buildup behaviour and its dependence on the experimental conditions, such as DFTL length, pumping rate, and pump pulse duration.

The time-dependent τ_c plays a key role in short pulse formation. It has a large value during the rising half of DFTL pulse and has a low value during the decaying half, which consequently favours the formation and shortening of the DFTL pulses. Such a mechanism of short pulse formation was called self Q-switching by Bor.[11] Another important effect which leads to the pulse buildup behaviour is the amplified spontaneous emission (ASE). The exact theoretical description of ASE is fairly complicated, but in this paper we give a gross estimate of the intensity of ASE to investigate its effects by numerical study. In previous solutions of DFTL, the spontaneous emission was neglected in all the pumping pulse period. Therefore, in the investigation of ASE effect, we should add this part to the coupled rate equations. This is done by estimating the values of photons intensity at an output wavelength from ASE and then setting this value as the lower bound of q in rate equations. The numerical solution indicates that ASE has a reverse effect of τ_c and exhibits the increase of pulse width, the decrease of pulse power, pulse buildup time, and the time separation between pulses (see Fig.5).

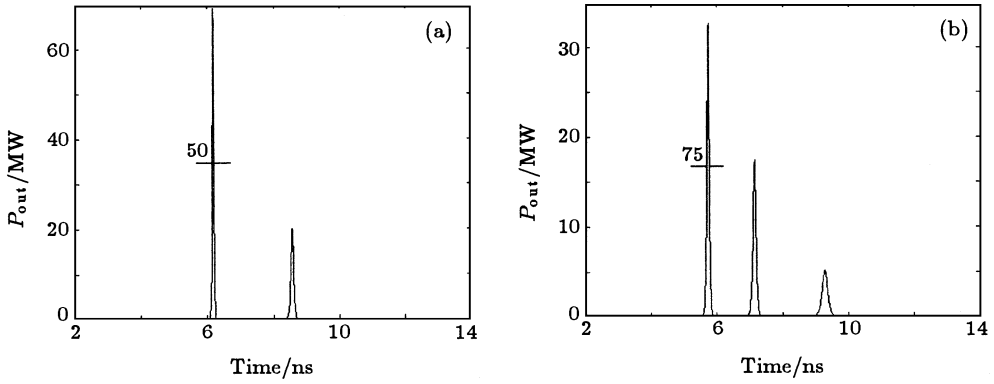


Fig.5. Comparison between resolutions of coupled rate equations (a) without ASE effect and (b) with ASE effect. The photon intensity at output wavelength from ASE is estimated as $10^{-8} \times n(t)$.

The output pulse duration under various experimental conditions can be predicted by numerical solution. We hereby study the effects of length of DFTL, pumping rates, and pumping pulse duration on it. The computer solutions predict a pulse broadening as the length of DFTL decreases. It is understandable from Eq.(12), that a shorter length of DFTL results in a larger value of n_{th}, and thus a larger bleaching effect of ground state, which has an effect of pulse broadening and peak power descending. The effects of pumping rates and pumping pulse duration are a little more complex. It seems that they have an incorporation effect on the output pulse duration. Figure 6 shows contour curves of the first output pulse duration corresponding to different pumping rates and pumping pulse duration. The points on contour curves with larger values stand for the output pulses with smaller peak power and pulse energy. The curve with largest value (stands for the output pulse on threshold condition) is very close to a contour curve pulse energy density (pumping rate multiplies pumping pulse duration). And near the threshold condition, the output pulse duration decreases rapidly with the increase

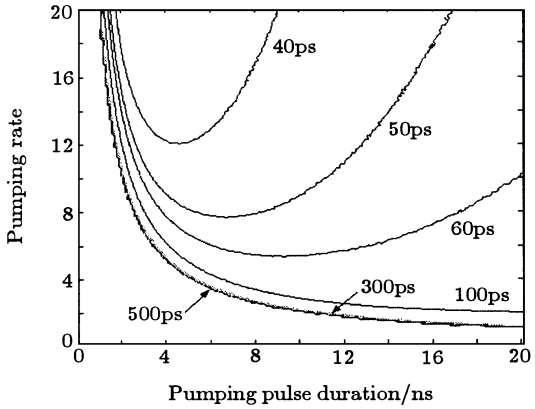


Fig.6. Calculated contour curves of output pulse duration. A unit of pumping rate equals $6.23 \times 10^{26}\text{cm}^{-3}\cdot\text{s}^{-1}$. The damage threshold of Ti:sapphire is ignored in this figure.

of pumping pulse energy density. From Fig.6 We also obtain the conclusion that there exists almost the same energy density threshold for different pumping pulse durations.

In terms of the generation of picosecond pulses, DFTL has some important advantages compared with the DFDL. It offers much higher output pulse energy. Single pulse energy with several mJ can be achieved without amplifier. And it is more stable and easier to be utilized due to its solid-state laser system.

4. Conclusions

In summary, a DFTL pumped by a 532nm Q-switched Nd:YAG laser is proposed for the generation of tunable picosecond pulses. The temporal characteristics of DFTL are obtained by solving the coupled rate equations. The numerical solutions show that the DFTL pulse with a 50-ps pulse duration and as much as 3.5mJ pulse energy can be obtained under 40mJ, 5ns pulse pumping. The dependence of output pulse width on the laser crystal length, pumping pulse duration, and pumping rate is also discussed in detail.

References

[1] Kollner M and Monkhouse P 1995 *Appl. Phys.* B **61** 499

[2] Ossler F, Larsson J and Alden M 1996 *Chem. Phys. Lett.* **250** 287

[3] Mori K, Morioka T and Saruwatari M 1993 *Electron. Lett.* **29** 987

[4] Rairoux P, Schillinger H, Niedermeler S, Rodriguez M, Ronneberger F, Sauerbrey R, Stein B, Waite D, Wedekind C, Wille H, Woste L and Ziener C 2000 *Appl. Phys.* B **71** 573

[5] Krainer L, Paschotta R, Shuhler G J, Klimov I, Teisset C Y, Weingarten K J and Keller U 2002 *Electron. Lett.* **38** 225

[6] Seitz W, Ell R, Morgner U, Schibli T R, Kartner F X, Lederer M J and Braun B 2002 *Opt. Lett.* **27** 2209

[7] Pashinin V P, Garnov S V, Konov V I, Senatorov A K and Sinyavskii M N 2002 *Quantum Electron.* **32** 121

[8] Spuhler G J, Paschotta R, Keller U, Moser M, Dymott M J P, Kopf D, Meyer J, Weingarten K J, Kmetec J D, Alexander J and Truong G 1999 *Opt. Lett.* **24** 528

[9] Rimington N W, Cornea A, Tassle A J V, Santoro J and Schroeder W A 2001 *Appl. Opt.* **40** 4831

[10] Wang Y S, Cheng G H, Liu Q, Sun C D, Zhao W and Chen G F 2004 *Acta Phys. Sin.* **53** 87 (in Chinese)

[11] Bor Zs 1980 *J. Quantum Electron.* **16** 517

[12] Voss T, Scheel D and Schade W 2001 *Appl. Phys.* B **73** 105

[13] Yaney P P, Kliner D A V, Schrader P E and Farrow R L 2000 *Rev. Sci. Instrum.* **71** 1296

[14] Shank C V, Bjorkholm J E and Kogelnik H 1971 *Appl. Phys. Lett.* **18** 395

[15] Hill K O and Watanabe A 1975 *Appl. Opt.* **14** 950

[16] Haus H A 1975 *Appl. Opt.* **14** 2650

[17] Chinn S R 1976 *Opt. Commun.* **19** 208